Carrier Redistribution in van der Waals Nanostructures Consisting of Bilayer Graphene and Buckybowl: Implications for Piezoelectric Devices

Mina Maruyama* and Susumu Okada

Department of Physics, Graduate School of Pure and Applied Sciences, University of Tsukuba, 1-1-1 Tennodai, Tsukuba, Ibaraki 305-8571, Japan

E-mail: mmaruyama@comas.frsc.tsukuba.ac.jp

Phone: +81 (0)29 8535921. Fax: +81 (0)29 8535924

Abstract

Geometric and electronic structures of a complex nanomaterial consisting of a sumanene ($C_{21}H_{12}$) and bilayer-graphene are investigated in terms of the molecular conformation between the layers with density functional theory. Our calculations indicated that the sumanene-intercalated bilayer-graphene is the key material for designing the piezoelectric devices capable of supplying an electric energy density of 30 μWh/cm^2. The dipole moment of a bowl-shaped hydrocarbon sumanene induces an electrostatic potential difference between the graphene layers resulting in charge transfer between the graphene layers. Holes and electrons are induced on the graphene layers located at the convex and edge sides of sumanene, respectively, with the densities of 4.4×10^{12} and 6.6×10^{11} /cm^2. Furthermore, the two-dimensional nano-spacing between the graphene layers changes the molecular conformation of sumanene from a bowl to flat structure at 0.8 GPa.

Introduction

Graphite occupies an important position in physical and chemical sciences owing to its unique structural and physical properties, which offer the potential for a wide variety of derivatives.[1,2] Fullerenes and carbon nanotubes have been synthesized by arc discharge with graphite electrodes.[3,4] These carbon allotropes have hollow-caged and tubular forms, respectively, and their unusual physical properties reflect their dimensionality, local atomic arrangement, and boundary conditions imposed on the hexagonal covalent network.[5,6] Mechanical exfoliation of bulk graphite and chemical vapor deposition of hydrocarbons on substrates can produce graphene, which is the ultimate two-dimensional electron system with atomic thickness.[7] Furthermore, recent advances in layer-by-layer growth techniques of graphene have enabled tailoring of the thickness and interlayer stacking arrangement of graphite. These structures are known as graphene thin films or few-layer graphene.[8,9] In particular, bilayer graphene has unusual electronic structures not seen in bulk graphite and isolated monolayer graphene. These unique features depend on the stacking arrangement and external electric field. Bilayer graphene with an AB stacking arrangement is a semiconductor under a vertical external electric field, and the band gap depends on the field strength.[10–13] In contrast, twisted bilayer graphene with a particular twist angle is a superconductor because of flat dispersion bands that arise from band repulsion owing to zone folding.[14]

In addition to the physics and chemistry associated with the honeycomb covalent networks and interlayer stacking arrangements, graphite is also regarded as an important host material for intercalation compounds with various guest atoms and molecules.[1,15] Those intercalation compounds are known as graphite intercalation compounds (GICs) and have a wide variety of physical properties that depend on the guest intercalants. Intercalation of alkaline and alkaline-earth elements enhances the transport properties of GICs,[16–19] depending on the stoichiometry and staged structure, through charge transfer from the intercalant atoms to graphite and hybridization between their electron states.[20,21] Magnetism has also been induced by intercalated atoms or molecules with spin polarization.[22] Furthermore, nanocarbon

materials, such as aromatic hydrocarbon molecules and fullerenes, can be accommodated in interlayer spaces of graphite.[23–28] These carbon-based intercalation compounds are potential candidates for all-carbon charge transfer complexes, because of the electron affinity differences of the constituents owing to their structures. As for the geometric structure of guest materials, these are two-dimensionally arranged within the nano-spaced interlayers, with different atomic or molecular arrangements from their bulk forms, which leads to unique physical properties.

By analogy with GICs, few-layered graphene or graphene thin films are host materials that can form such complexes by accommodation of foreign atoms or molecules as an ultimate version of GICs.[29,30] In complexes derived from few-layered graphene, the surfaces above and below the graphene thin films contribute to physical properties that are absent in typical GICs composed of bulk graphite, although they contain the same guest atoms or molecules. For instance, guest molecules with a dipole moment may cause symmetry breaking between the graphene layers leading to formation of a band gap, as occurs in the case of bilayer graphene under an electric field.

Therefore, in this manuscript, we aimed to explore the geometric and electronic structures of an intercalation compounds comprising bilayer graphene and a bowl-shaped polycyclic hydrocarbon molecule as a potential carbon-based intercalation compounds with unique electronic properties, based on the density functional theory.[31,32] Our calculations reveal that the sumanene molecule ($C_{21}H_{12}$)[33–35] intercalated in bilayer graphene induces charge transfer between the graphene layers owing to the electron polarization in the molecule: Formation of holes and electrons is induced by sumanene intercalation and these distribute at the top and bottom graphene layers with densities of 4.4 $\times 10^{12}$ and 6.6×10^{11} /cm^2, respectively. Furthermore, we demonstrate that the two-dimensional nano-spacing between the graphene layers changes the molecular conformation of sumanene from bowl to flat under a compression of 0.8 GPa. Therefore, sumanene-intercalated bilayer-graphene has potential application in piezoelectric devices capable of supplying an electric energy density of 30

μWh/cm^2.

Results and discussion

In this work, we considered the sumanene molecule ($C_{21}H_{12}$) as a guest intercalant in bilayer graphene to explore a potential carbon-based intercalation compounds with unique geometric and electronic structures. Owing to its bowl-shaped molecular conformation with edges terminated by H atoms, sumanene has a dipole moment normal to the bowl which can modulate the electronic structure of the graphene layers even though the molecule has a deep highest occupied and shallow lowest unoccupied states. Furthermore, sumanene on a Au(111) surface undergoes a bowl-to-bowl conversion via a flat conformation, as observed by scanning tunneling microscopy, with an energy barrier of 0.8 eV.[36,37] The barrier is approximately same as the energy difference between the bowl and flat conformations. The calculated energy difference is 0.83 eV between isolated sumanene with bowl and flat conformation. This result suggests the possibility of electron state tuning of the bilayer graphene intercalation compounds under uniaxial pressure.

Figure 1 shows optimized geometric structures of sumanene-intercalated bilayer-graphene. Sumanene is intercalated in bilayer graphene with an AA stacking arrangement of 5×5 lateral periodicity where sumanene is separated from its adjacent molecules by 3.88 and 3.32 Å for bowl and flat molecular conformations, respectively. Calculated molecular thickness of sumanene with bowl conformation in bilayer graphene is 1.13 Å which is evaluated by taking the difference between z coordinates of C belonging to center and edge of sumanene. Note that the value is the same as that of an isolated sumanene molecule. Indeed, the maximum force acting on C atoms in complexes is less than 2×10^{-3} Hartree/a.u., ensuring the flatness of graphene and bowl shape of sumanene. The optimum spacing between the convex part of the sumanene and graphene is 3.1 Å for the bowl shape conformation, whereas the spacing between the edge H atom and graphene is 2.6 Å for both molecular conformations. Our

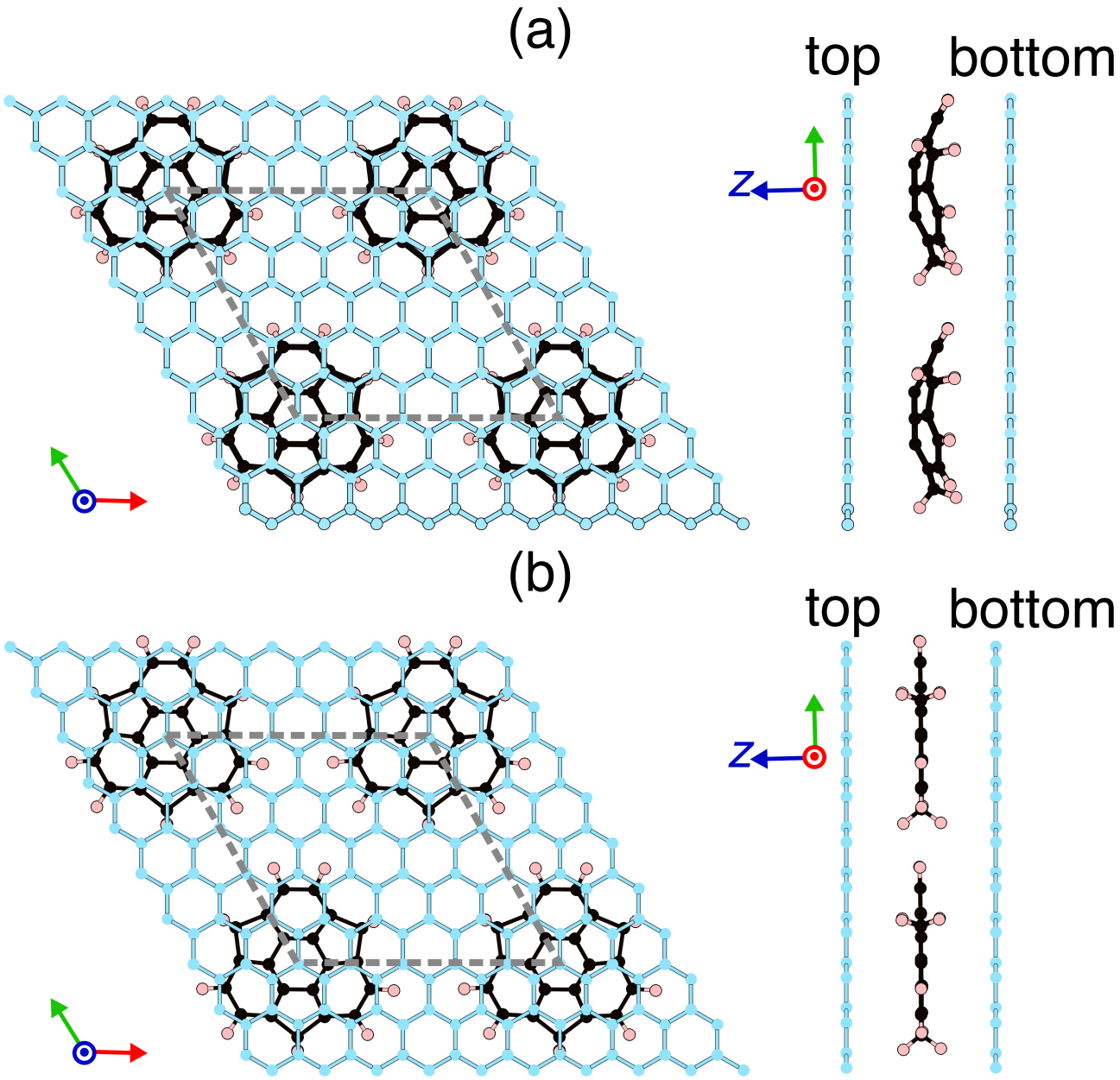

Figure 1: Top and side views of geometric structures of bilayer graphene with AA stacking arrangement intercalating sumanene with (a) bowl and (b) flat conformations. Black, pink, and blue circles indicate C atoms of sumanene, H atoms of sumanene, and C atoms of graphene, respectively. Gray dotted parallelograms denote the lateral super cell of sumanene intercalated 5 × 5 bilayer graphene.

calculations show that sumanene with a bowl conformation intercalated in bilayer graphene is more stable than that with a flat conformation by 0.42 eV. Notably, this value is approximately half of the experimentally observed energy barrier for bowl-to-bowl conversion on Au(111) surfaces and our theoretical estimation on an isolated sumanene. It is worth to discuss the energetics of the complex in terms of the mutual orientation of sumanene. The total energy of the complexes with bowl conformation depended on the mutual angle by energy of 93 meV per cell (Figure S1). Thus, the energy difference between the bowl and flat conformations may slightly change by the energy of approximately 0.1 eV depending on their mutual orientation to the graphene layers. These results indicate that the nanoscale two-dimensional spacing between graphene greatly stabilizes the flat conformation of sumanene. It is also notable that further dynamical phenomena are expected under the finite temperature.

Figure 2a and 2b show the electronic structures of sumanene with bowl and flat conformations, respectively, intercalated in bilayer graphene. Thus, the sumanene-intercalated bilayer-graphene is a metal possessing Dirac cones around and at the Fermi level for both molecular conformations. The energy bands associated with the highest occupied and the lowest unoccupied states of sumanene are, respectively, located 1 eV below and 2 eV above the Fermi level, indicating that there is no possibility for charge transfer between sumanene and graphene. However, in the case of sumanene-intercalated bilayer-graphene with a bowl conformation, two Dirac cones split into upper and lower cones with an energy difference of 0.54 eV at the K point (Figure 2a). This Dirac cone splitting may enable electron transfer from the upper Dirac cone to the lower one, leading to electron and hole co-doping into the bilayer graphene intercalation compound consisting of carbon atoms. In contrast, sumanene-intercalated bilayer-graphene with a flat conformation has a doubly degenerate Dirac cone at the Fermi level, indicating that charge transfer is absent (Figure 2b).

To investigate the physical origin of the Dirac cone splitting, we investigated the wave function distribution of Kohn-Sham orbitals in the Dirac cones of sumanene-intercalated bilayer-graphene (Figure 3). For the bilayer-graphene intercalating bowl shaped sumanene,

the wave functions of the upper and lower Dirac cones were distributed in layers located at the convex and edges sides of sumanene, respectively, both with π state character similar to that of an isolated graphene layer (Figure 3a). This result confirms that holes and electrons are injected into the graphene layers at the convex and edges sides, respectively. For the sumanene-intercalated bilayer-graphene with a flat conformation, a wave function associated with the degenerate Dirac cones is distributed over both graphene layers with π state character (Figure 3b).

Figure 4 shows the charge density difference in sumanene-intercalated bilayer-graphene with a bowl conformation upon the sumanene interaction. The charge density difference, $\Delta\rho(\boldsymbol{r})$, is evaluated by the equation,

$$\Delta\rho(\boldsymbol{r}) = \rho_{\mathrm{BGC}}(\boldsymbol{r}) - \rho_{\mathrm{BLG}}(\boldsymbol{r}) - \rho_{\mathrm{suma}}(\boldsymbol{r}) \tag{1}$$

where $\rho_{\mathrm{BGC}}(\boldsymbol{r})$, $\rho_{\mathrm{BLG}}(\boldsymbol{r})$, and $\rho_{\mathrm{suma}}(\boldsymbol{r})$ are charge densities of sumanene-intercalated bilayer-graphene, an isolated bilayer graphene with large interlayer spacing, and an isolated sumanene molecule, respectively. The charge density difference indicates that electrons transfer from the top graphene layer to the bottom layer. Holes are injected into the top graphene layer at the convex side, whereas electrons and holes are induced at the bottom layer near the edges of sumanene (Figure 4a). By integrating the charge density in planes parallel to graphene layers, we found that holes and electrons are primarily induced at the top and bottom layers of graphene, respectively (Figure 4b). Furthermore, by taking the sum of the charge density by shaded areas in Figure 4b, we can evaluate the carrier concentration in graphene layers. The hole and electron densities at the top and bottom layers are 4.4×10^{12} and $6.6\times10^{11}/\mathrm{cm}^2$, respectively. The carrier concentration is lower than that in K-GIC ($\sim 2\times10^{14}$ /cm^2), but comparable to those in conventional semiconductors ($10^{12} \sim 10^{13}$ /cm^2). In addition to the electron and hole injection into graphene layers, charge redistribution occurs in sumanene molecules where the electrons and holes are induced in the convex region of sumanene and

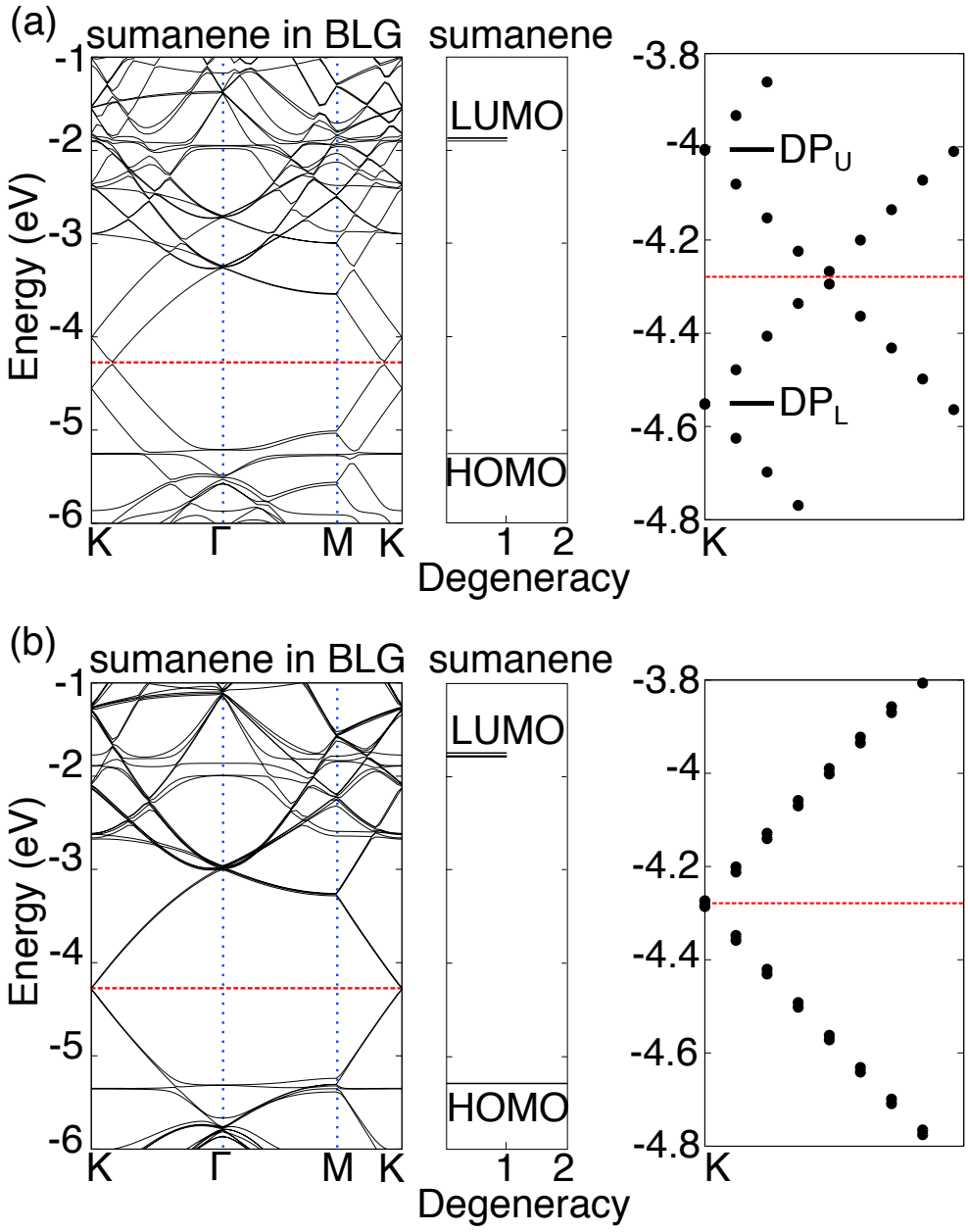

Figure 2: Electronic band structures of sumanene-intercalated bilayer-graphene with (a) bowl and (b) flat conformations. Vertical blue and horizontal red doted lines denote the symmetric points in reciprocal space and the Fermi level, respectively. Electronic structures of an isolated sumanene molecule with bowl and flat conformations are also shown in a middle panel of each figure. The labels of degeneracy 1 and 2 indicate the non-degenerated and doubly degenerated states, respectively. Enlarged band structures near the Fermi level and the K point are shown in a right panel in each figure. Labels DP_U and DP_L indicate the upper and lower Dirac points split by the intercalation of sumanene with bowl conformation. Energy is measured from that of the vacuum level.

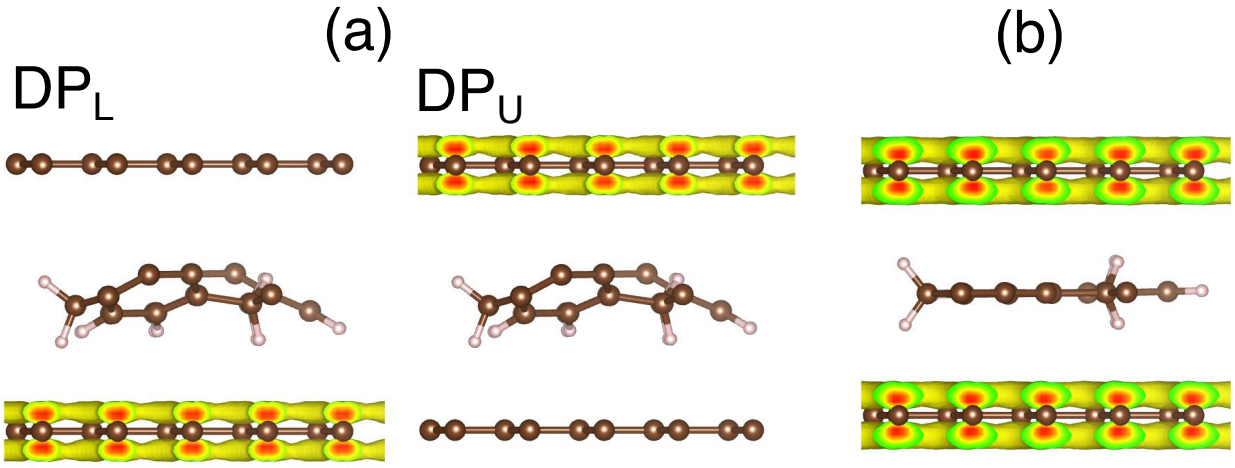

Figure 3: Isosurfaces of squared wave function of Kohn-Sham orbitals of Dirac cones at the K point of sumanene-intercalated bilayer-graphene with (a) bowl and (b) flat conformations. Labels in (a) correspond with those in Figure 2.

the edge H atoms, respectively.

The Dirac cone splitting of 0.54 eV suggests that the electron and hole doping in the bilayer graphene is attributed to the dipole moment of sumanene sandwiched between the layers. To clarify the physical origin of charge transfer between top and bottom graphene layers, we investigated the electrostatic potential of sumanene-intercalated bilayer-graphene with a bowl-shape conformation (Figure 5a). The electrostatic potential at the top vacuum is higher than that at the bottom vacuum by 0.55 V which is approximately the same as the Dirac cone splitting. According to this potential difference, electrons are transferred from the top graphene layer to the bottom graphene layer, resulting in holes residing at the top layer and electrons in the bottom layer. The potential difference between upper and lower layers of graphene implied the dipole moment of sumanene sandwiched in them. Indeed, the calculated dipole moment of sumanene is 1.3 D. Therefore, the molecular dipole moment is the physical origin of the induced charge transfer between the graphene layers owing to the electrostatic potential difference between layers. Notably, the concave region of sumanene had a higher potential profile than that induced by the C-H polarization at the edge atomic sites. It is obvious that the potential difference between graphene layers is absent for sumanene with

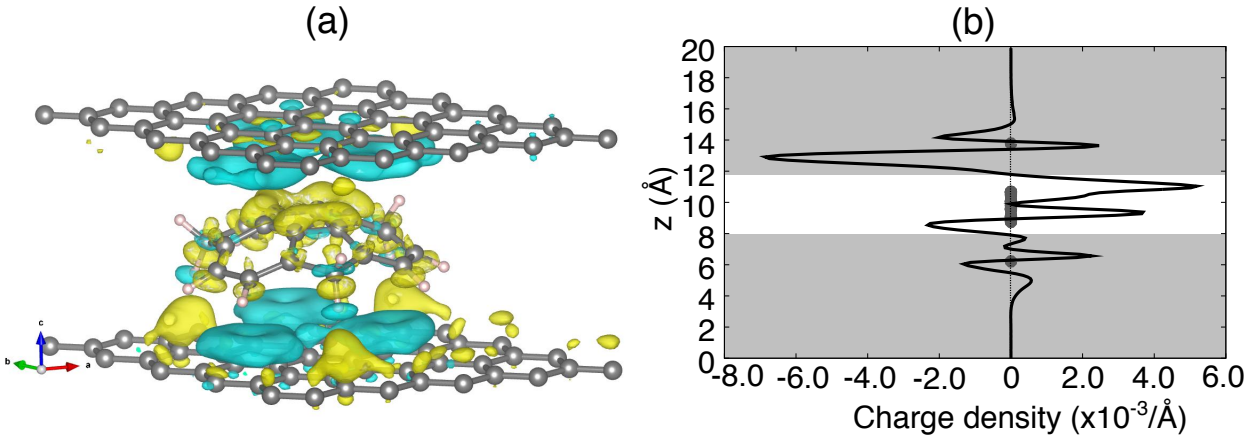

Figure 4: (a) Isosurfaces of charge density differences of sumanene-intercalated bilayer-graphene with bowl conformation. Blue and yellow isosurfaces indicate hole and electron distributions, respectively. Isosurfaces indicate the charge density of $\pm$ 0.0013 e/Å^3. Gray and white balls indicate C and H atoms, respectively. (b) Charge density distribution normal to the graphene layers and sumanene. Positive and negative values correspond to the regions of electron accumulation and depression, respectively. Gray points denote atomic positions. Shaded areas correspond the region belonging to graphene layers.

flat conformation in bilayer graphene (Figure 5b). The electrostatic potential exhibited a symmetric nature with respect to the middle of upper and lower graphene layers.

We discuss the possibility of a structural transformation of sumanene from a bowl to flat conformation within the graphene layers, because of the substantial decrease of the energy difference between these two conformations within the intercalated structure. Figure 6 shows the total energy of the sumanene-intercalated bilayer-graphene as a function of interlayer spacing. A bowl conformation is the ground state conformation between the graphene layers and is 0.42 eV/molecule lower in energy than that is the flat conformation. Since the free energy of the system is expressed as $F = U - TS$ where U corresponds with the calculated total energy, S is the entropy, and T is the temperature, we can discuss the pressure inducing phase transition on the complex under 0K, using the energy curves shown in Figure 6. By calculating a common tangential line for both energy curves ($P = \frac{1}{S_{uc}}\frac{\partial F}{\partial z} = \frac{1}{S_{uc}}\frac{\partial U}{\partial z}$ where S_{uc} is the area of the unit cell) which are obtained by polynomial fitting up to fifth order of z, we can conclude that possibility of a structural phase transition on the intercalated sumanene from bowl to flat molecular conformations under a critical pressure of $P_c = 0.8$

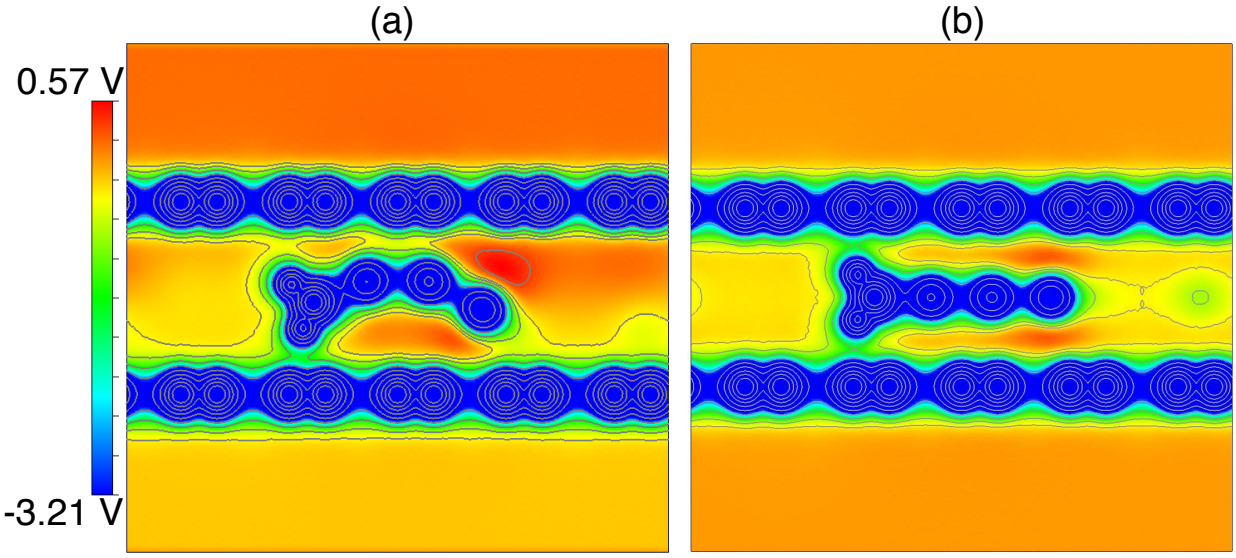

Figure 5: Contour plot of the electrostatic potential of sumanene-intercalated bilayer-graphene with (a) bowl and (b) flat conformations on the plane normal to the graphene layers and sumanene. Red and blue colors indicate regions of high and low electrostatic potential, respectively. Each contour line represents twice (or half) the density of the adjacent contour lines.

GPa. It should be noted that the stacking arrangement of graphene layers may decrease the transition pressure. Because the energy of sumanene with the bowl conformation in bilayer graphene with AA stacking is the same as that in bilayer graphene with AB stacking, while that of sumanene with flat conformation in bilayer graphene with AA is higher by 97 meV than that in bilayer graphene with AB stacking.

Therefore, mechanical strain applied normal to the graphene layers can control the carrier density and polarity of sumanene-intercalated bilayer-graphene. This result could be potentially harnessed to develop piezoelectric devices supplying an electric energy density of 30 μWh/cm^2, as evaluated from the carrier density and potential difference between the layers. For such applications, the orientation of sumanene will determine the device stability. Layer-by-layer deposition techniques may be used to control the sumanene orientation between graphene layers, because graphene prefers sumanene edges compared with the convex region with an energy difference of 30 meV. This approach will overcome the energy gain owing to the dipole-dipole interaction between adjacent sumanene with a staggered

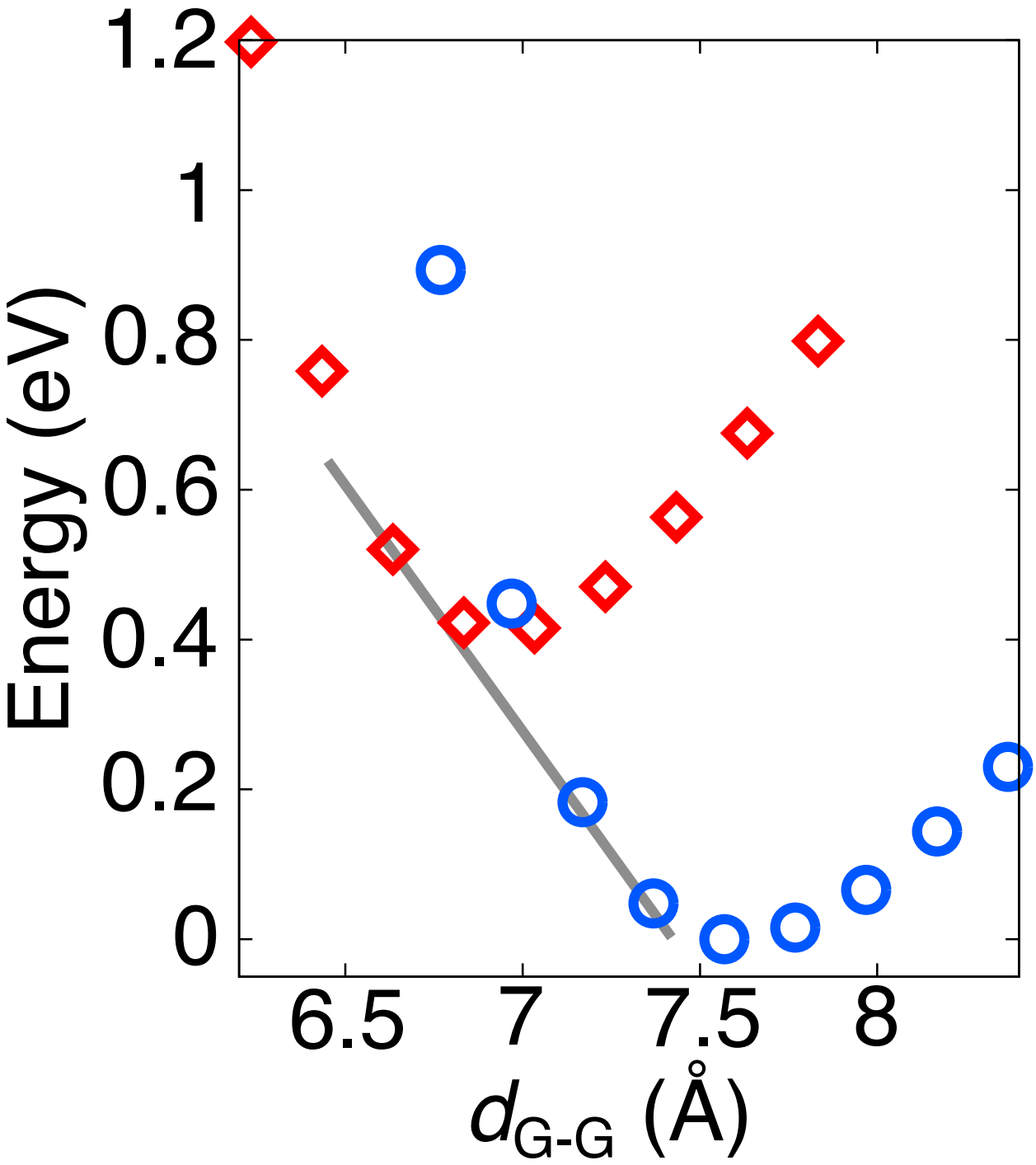

Figure 6: Calculated total-energy of sumanene-intercalated bilayer-graphene as a function of interlayer spacing of bilayer graphene, d_{G-G}. Blue circles and red rhombuses indicate the energy of sumanene-intercalated bilayer-graphene with bowl and flat conformations, respectively. Energies are measured form the ground state energy of sumanene-intercalated bilayer-graphene with bowl conformation. Gray line denotes a common tangential line between two energy curves of sumanene-intercalated bilayer-graphene with bowl and flat conformations.

molecular conformation (7 meV at a sumanene-sumanene distance of 7 Å). Even though the sumanene forms staggered conformation between graphene layers, an external electric field perpendicular to the molecules can flip and align its bowl direction (Figure S2)

Conclusion

On the basis of density functional theory with the generalized gradient approximation, we theoretically investigate the geometric and electronic structures of a carbon-based intercalation compound comprising bilayer graphene and a bowl-shaped hydrocarbon sumanene, as the thinnest potential graphite intercalation compound. Owing to electron and hole co-doping of the bilayer graphene under equilibrium conditions and the conformation change of sumanene under pressure, sumanene-intercalated bilayer-graphene is potentially applicable in piezoelectric devices capable of supplying an electric energy density of 30 μWh/cm^2. The dipole moment normal to molecular plane of sumanene causes an electrostatic potential difference between graphene layers when sumanene is intercalated into the interlayer spacing of bilayer graphene. The Dirac cones split into upper and lower cones reflecting the potential difference between the layers, such that the splitting induces opposing carriers in the graphene layers. Hole and electron densities of 4.4×10^{12} and 6.6×10^{11}/cm^2 are induced on the graphene layers situated at the convex and edge sides of intercalated sumanene, respectively. Intercalation also decreases the energy difference between sumanene with bowl and flat conformations by half, so that sumanene has a flat conformation in the interlayer spacing of bilayer graphene under a uniaxial pressure of 0.8 GPa.

Methods

The geometric and electronic structure of sumanene-intercalated bilayer-graphene were investigated using the STATE package based on density functional theory.[38,39] For the exchange-correlation potential energy among interacting electrons, the generalized gradient approxima-

tion was used with the functional forms of Perdew–Burke–Ernzerhof.[40–42] The dispersive interaction between sumanene and graphene was treated by vdW-DF2 with the C09 exchange-correlation functional.[43,44] An ultrasoft pseudopotential was used to describe electron–ion interactions.[46] A plane-wave basis set with the cutoff energies of 25 and 225 Ry was adopted to expand the valence wave functions and deficit charge density, respectively. Note that the above cutoff energy gives enough convergence in relative energy of carbon related materials within energy of 1 meV/atom. Self-consistent electronic structure calculations were conducted with 4×4×1 $\boldsymbol{k}$-meshes for sumanene-intercalated bilayer-graphene with 5×5 lateral periodicity. Structural optimization was performed until the remaining forces on each atom were less than 5 mRy/Å. Because an intrinsic dipole moment normal to the molecular plane of sumanene is expected to occur, we adopted the effective screening medium method (ESM) to avoid an unphysical dipole interaction with those in imaging cells normal to the sumanene-intercalated bilayer-graphene, separated by a vacuum spacing of at least 10 Å, under periodic boundary conditions.[47] In the ESM, we adopted an open boundary condition with respect to the electrostatic properties normal to the graphene layers by considering Poisson's equation

$$[\frac{\partial}{\partial z}\epsilon(z)\frac{\partial}{\partial z} - \epsilon(z)g_{\parallel}^2]V(\boldsymbol{g}_{\parallel}, z) = -4\pi\rho(\boldsymbol{g}_{\parallel}, z),$$

where $\epsilon(z)$, $V(\boldsymbol{g}_{\parallel}, z)$, $\boldsymbol{g}_{\parallel}$, and ρ indicate the relative permittivity, electrostatic potential, wave number vector parallel to layers, and charge density, respectively, under the following conditions of $\frac{\partial}{\partial z}V(\boldsymbol{g}_{\parallel}, z)|_{z=\pm\infty} = 0$ and $\epsilon(z) = 1$.

Acknowledgement

The authors thank JST-CREST Grant Numbers JPMJCR20B5, JPMJCR1532, and JPMJCR1715 from the Japan Science and Technology Agency, JSPS KAKENHI Grant Numbers JP20H05664, JP20K05253, JP20H02080, JP20H00316, and JP16H06331 from the Japan Society for the Promotion of Science, the Joint Research Program on Zero-Emission Energy

Research, Institute of AdvancedEnergy, Kyoto University, and University of Tsukuba Basic Research Support Program (S). Part of the calculations was performed on an NEC SX-Ace at the Cybermedia Center, Osaka University.

References

(1) Dresselhaus, M. S.; Dresselhaus, G. Intercalation Compounds of Graphite. Adv. Phys. 1981, 30, 139–326.

(2) Castro Neto, A. H.; Guinea, F.; Peres, N. M. R.; Novoselov, K. S.; Geim, A. K. The Electronic Properties of Graphene. Rev. Mod. Phys. 2009, 81, 109–162.

(3) Kroto, H. W.; Heath, J. R.; O'Brien, S. C.; Curl, R. F.; Smalley, R. E. C_{60}: Buckminsterfullerene. Nature 1985, 318, 162–163.

(4) Iijima, S. Helical Microtubules of Graphitic Carbon. Nature 1991, 354, 56–58.

(5) Saito, S.; Oshiyama, A. Cohesive Mechanism and Energy Bands of Solid C_{60}. Phys. Rev. Lett. 1991, 66, 2637–2640.

(6) Hamada, N.; Sawada, S.-I.; Oshiyama, A. New One-dimensional Conductors: Graphitic Microtubules. Phys. Rev. Lett. 1992, 68, 1579–1581.

(7) Novoselov, K. S.; Geim, A. K.; Morozov, S. V.; Jiang, D.; Zhang, Y.; Dubonos, S. V.; Grigorieva, I. V.; Firsov, A. A. Electric Field Effect in Atomically Thin Carbon Films. Science 2004, 306, 666–669.

(8) Masubuchi, S.; Morimoto, M.; Morikawa, S.; Onodera, M.; Asakawa, Y.; Watanabe, K.; Taniguchi, T.; Machida, T. Autonomous Robotic Searching and Assembly of Two-dimensional Crystals to Build van der Waals Superlattices. Nat. Commun. 2018, 9, 1413.

(9) Masubuchi, S.; Watanabe, E.; Seo, Y.; Okazaki, S.; Sasawaga, T.; Watanabe, K.; Taniguchi, T.; Machida, T. Deep-learning-based Image Segmentation Integrated with Optical Microscopy for Automatically Searching for Two-dimensional Materials, npj 2D Mater. Appl. 2020, 4, 3.

(10) McCann, E. Asymmetry Gap in the Electronic Band Structure of Bilayer Graphene. Phys. Rev. B 2006, 74, 161403.

(11) Castro, E. V.; Novoselov, K. S.; Morozov, S. V.; Peres, N. M. R.; Lopes dos Santos, J. M. B.; Nilsson, J.; Guinea, F.; Geim, A. K.; Castro Neto, A. H. Biased Bilayer Graphene: Semiconductor with a Gap Tunable by the Electric Field Effect, Phys. Rev. Lett. 2007, 99, 216802.

(12) Oostinga, J. B.; Heersche, H. B.; Liu, X.; Morpurgo, A. F.; Vandersypen, L. M. K. Gate-induced Insulating State in Bilayer Graphene Devices. Nat. Mater 2008, 7, 151–157.

(13) Otani, M.; Okada, S. Field-induced Free-electron Carriers in Graphite. J. Phys. Soc. Jpn. 2010, 79, 073701.

(14) Cao, Y.; Fatemi, V. Fang, S.; Watanabe, K.; Taniguchi, T.; Kaxiras, E.; Jarillo-Herrero, P. Unconventional Superconductivity in Magic-angle Graphene Superlattices, Nature 2018, 556, 43–50.

(15) Enoki, T.; Suzuki, M.; Endo, M. Graphite Intercalation Compounds and Applications; Oxford University Press: New York, 2003.

(16) Koma, A.; Miki, K.; Suematsu, H.; Ohno, T.; Kamimura, H. Density-of-states Investigation of C_8K and Occurrence of the Interlayer Band. Phys. Rev. B 1986, 34, 2434–2439.

(17) Parry, G. S.; Nixon, D. E. Order-disorder Transformation in Potassium Graphite. Nature 1967, 216, 909–910.

(18) Metrot, A.; Guerard, D.; Bikkaud, D.; Herold, A. New Results About the Sodium-graphite System, Synth. Met. 1980, 1, 363–369.

(19) Weller, T. E.; Ellerby, M.; Saxena, S. S.; Smith, R. P.; Skipper, N. T. Superconductivity in the Intercalated Graphite Compounds C_6Yb and C_6Ca, Nat. Phys. 2005, 1, 39–41.

(20) Posternak, M.; Baldereschi, A.; Freeman, A. J.; Wimmer, E.; Weinert, M. Prediction of Electronic Interlayer States in Graphite and Reinterpretation of Alkali Bands in Graphite Intercalation Compounds, Phys. Rev. Lett. 1983, 50, 761–764.

(21) Posternak, M.; Baldereschi, A.; Freeman, A. J.; Wimmer, E. Prediction of Electronic Surface States in Layered Materials: Graphite. Phys. Rev. Lett. 1984, 52, 863–866.

(22) Suematsu, H.; Ohmatsu, K.; Sakakibara, T.; Date, M.; Suzuki, M. Magnetic Properties of Europium-graphite Intercalation Compound C_6Eu. Synth. Met. 1983, 8, 23–30.

(23) Beǵuin, F.; Setton, R.; Facchini, L.; Legrand, A. P.; Merle, G.; Mai, C. Structure and Properties of $KC_{24}(Bz)_2$, A graphite-potassium-benzene Intercalation Compound. Synth. Met. 1980, 2, 161–170.

(24) Isaev, Y. V.; Novikov, Y. N.; Vol'pin, M. E.; Rashkov, I.; Panayotov, I. Ternary Lamellar Graphite Compounds with Potassium and Methylbenzenes. Synt. Met. 1983, 6, 9–14.

(25) Jegoudez, J.; Mazieres, C.; Setton, R. Behaviour of the Binary Graphite Intercalation Compounds KC_8 and KC_{24} Towards a Set of Sample Organic Molecules. Synth. Met. 1983, 7, 85–91.

(26) Saito, S.; Oshiyama, A. Design of C_{60}-graphite Cointercalation Compounds. Phys. Rev. B 1994, 49, 17413–17419.

(27) Rut'kov, E. V.; Tontegode, A. Y.; Usufov, M. M. Evidence for a C_{60} Monolayer Intercalated between a Graphite Monolayer and Iridium. Phys. Rev. Lett. 1995, 74, 758–760.

(28) Gupta, V.; Scharff, P.; Risch, K.; Romanus, H.; Muller, R. Synthesis of C_{60} Intercalated Graphite. Solid State Commun. 2004, 131, 153–155.

(29) Kinoshita, H.; Jeon, I.; Maruyama, M.; Kawahara, K.; Terao, Y.; Ding, D.; Matsumoto, R.; Matsuo, Y.; Okada, S.; Ago, H. Highly Conductive and Transparent Large-area Bilayer Graphene Realized by $MoCl_5$ Intercalation. Adv. Mater. 2017, 29, 1702141.

(30) Kanahashi, K.; Tanaka, N.; Shoji, Y.; Maruyama, M.; Jeon, I.; Kawahara, K.; Ishihara, M.; Hasegawa, M.; Ohta, H.; Ago, at al.; Formation of Environmentally Stable Hole-doped Graphene Films with Instantaneous and High-density Carrier Doping via a Boron-based Oxidant, npj 2D Mater. Appl. 2019, 3, 7.

(31) Hohenberg P.; Kohn, W. Inhomogeneous Electron Gas. Phys. Rev. 1964, 136, B864–B871.

(32) Kohn W.; Sham, L. J. Self-Consistent Equations Including Exchange and Correlation Effects. Phys. Rev. 1965, 140, A1133–A1138.

(33) Higashibayashi, S.; Tsuruoka, R.; Soujanya, Y.; Purushotham, U.; Sadtry, G. N.; Seki, S.; Ishikawa, T.; Toyota, S.; Sakurai, H. Trimethylsumanene: Enantioselective Synthesis, Substituent Effect on Bowl Structure, Inversion Energy, and Electron Conductivity. Bull. Chem. Soc. Jpn. 2012, 85, 450–467.

(34) Sakurai, H.; Daiko, T.; Skane, H.; Amaya, T.; Hirao, T. Structural Elucidation of Sumanene and Generation of Its Benzylic Anions. J. Am. Chem. Soc. 2005, 127, 11580–11581.

(35) Amaya, T.; Seki, S.; Moriuchi, T.; Nakamoto, K.; Nakata, T.; Sakane, H.; Saeki, A.;

Tagawa, S.; Hirao, T. Anisotropic Electron Transport Properties in Sumanene Crystal. J. Am. Chem. Soc. 2009, 131, 408–409.

(36) Shrestha, B. B.; Karanjit, S.; Higashibayashi, S.; Sakurai, H. Correlation between Bowl-inversion Energy and Bowl Depth in Substituted Sumanenes. Pure Appl. Chem. 2014, 86, 747–753.

(37) Fujii, S.; Ziatdinov, M.; Higashibayashi, S.; Sakurai, H.; Kiguchi, M. Bowl Inversion and Electronic Switching of Buckybowls on Gold, J. Am. Chem. Soc. 2016, 138, 12142–12149.

(38) Morikawa, Y.; Iwata, K.; Terakura, K. Theoretical Study of Hydrogenation Process of Formate on Clean and Zn Deposited Cu(111) Surfaces. Appl. Surf. Sci. 2001, 169–170, 11–15.

(39) https://state-doc.readthedocs.io/en/latest/index.html

(40) Perdew, J. P.; Burke, K.; Ernzerhof, M. Generalized Gradient Approximation Made Simple. Phys. Rev. Lett. 1996, 77, 3865–3868.

(41) Perdew, J. P.; Burke, K.; Ernzerhof, M. Generalized Gradient Approximation Made Simple [Phys. Rev. Lett. 77, 3865 (1996)]. Phys. Rev. Lett. 1997, 78, 1396.

(42) Koda, D. S.; Bechstedt, F.; Marques, M.; Teles, L. K. Tuning Electronic Properties and Band Alignments of Phosphorene Combined with $MoSe_2$ and WSe_2. J. Phys. Chem. C 2017, 121, 3862–3869.

(43) Lee, K.; Murray, É. D.; Kong, L.; Lundqvist, B. I.; Langreth, D. C. Higher-accuracy van der Waals density functional. Phys. Rev. B 2010, 82, 081101(R).

(44) Cooper, V. R. Van der Waals Density Functional: An Appropriate Exchange Functional. Phys. Rev. B 2010, 81, 161104(R).

(45) Hamamoto, Y.; Hamada, I., Inagaki, K.; Morikawa, Y. Self-consistent van der Waals Density Functional Study of Benzene Adsorption on Si(100). Phys. Rev. B 2016, 93, 245440.

(46) Vanderbilt, D. Soft Self-Consistent Pseudopotentials in a Generalized Eigenvalue Formalism. Phys. Rev. B 1990, 41, 7892–7895.

(47) Otani, M.; Sugino, O. First-Principles Calculations of Charged Surfaces and Interfaces: A Plane-Wave Nonrepeated Slab Approach. Phys. Rev. B 2006, 73, 115407.

TOC Graphic